International Journal of Hydrogen Energy 95 (2024) 1261–1273

Contents lists available at ScienceDirect

International Journal of Hydrogen Energy

journal homepage: www.elsevier.com/locate/he

Towards the design of a hydrogen-powered ferry for cleaner passenger transport

G. Di Ilio [a,i,*], A. Bionda [b], R. Ponzini [c], F. Salvadore [d], V. Cigolotti [e,i], M. Minutillo [f,i], C. Georgopoulou [g], K. Mahos [h]

[a] University of Naples "Parthenope", Department of Engineering, Naples, Italy
[b] Politecnico di Milano, Department of Design, Milan, Italy
[c] CINECA – HPC Department, Milan office, Italy
[d] CINECA – HPC Department, Rome office, Italy
[e] ENEA - Italian National Agency for New Technologies, Energy and Sustainable Economic Development, Naples, Italy
[f] University of Salerno, Department of Industrial Engineering, Salerno, Italy
[g] DNV, Piraeus, Greece
[h] Levante Ferries, Athens, Greece
[i] ATENA Future Technology, Naples, Italy

ARTICLE INFO

Handling editor: Mehran Rezaei

Keywords:
Hydrogen-fueled ship
Fuel cells
Zero-emissions maritime transport
Virtual towing tank

ABSTRACT

The maritime transportation sector is a large and growing contributor of greenhouse gas and other emissions. Therefore, stringent measures have been taken by the International Maritime Organization to mitigate the environmental impact of the international shipping. These lead to the adoption of new technical solutions, involving clean fuels, such as hydrogen, and high efficiency propulsion technologies, that is, fuel cells.

In this framework, this paper proposes a methodological approach aimed at supporting the retrofit design process of a car-passenger ferry, operating in the Greece's western maritime zone, whose conventional powertrain is replaced with a fuel cell hybrid system. To this aim, first the energy/power requirements and the expected hydrogen consumption of the vessel are determined basing on a typical operational profile, retrieved from data provided by the shipping company. Three hybrid powertrain configurations are then proposed, where fuel cell and batteries are balanced out according to different design criteria. Hence, a new vessel layout is defined for each of the considered options, by taking into account on-board weight and space constraints to allocate the components of the new hydrogen-based propulsion systems. Finally, the developed vessel configurations are simulated in a virtual towing tank environment, in order to assess their hydrodynamic response and compare them with the original one, thus providing crucial insights for the design process of new hydrogen-fueled vessel solutions.

Findings from this study reveal that the hydrogen-based configurations of the vessel are all characterized by a slight reduction of the payload, mainly due to the space required to allocate the hydrogen storage system; instead, the hydrodynamic behavior of the H_2 powered vessels is found to be similar to the one of the original Diesel configuration; also, from a hydrodynamic point of view, the results show that mid load operating conditions get relevance for the design process of the hybrid vessels.

List of abbreviations

CFD	Computational Fluid Dynamics	ITTC	International Towing Tank Committee
DoD	Depth of Discharge	LH2	Liquid Hydrogen
DoF	Degrees of Freedom	LHV	Lower Heating Value
EM	Electric Motor	LSFO	Low Sulphur Fuel Oil
FC	Fuel Cell	MGO	Marine Gasoil
FGSS	Fuel Gas Supply System	PEM	Polymer Electrolyte Membrane
GHG	Greenhouse Gases	RANS	Reynolds Averaged Navier-Stokes

(continued on next column)
(continued)
(continued on next page)

* Corresponding author. University of Naples "Parthenope", Department of Engineering, Naples, Italy.
E-mail address: giovanni.diilio@uniparthenope.it (G. Di Ilio).

https://doi.org/10.1016/j.ijhydene.2024.08.434
Received 30 April 2024; Received in revised form 12 August 2024; Accepted 27 August 2024
Available online 6 September 2024

(*continued*)

HPC	High Performance Computing	RoPax	Roll-on/Roll-off passenger
ICE	Internal Combustion Engine	RoRo	Roll-on/Roll-off
IMO	International Maritime Organization	VoF	Volume of Fluid

1. Introduction

The maritime sector is a main pillar of global economy, as the majority of the world's trade is made by ships. Along with the transportation of goods, the passenger shipping is a prominent economic activity as well. The total number of passengers embarked and disembarked in EU ports was 348.6 million in 2022, with the Greece being the largest maritime passenger transport country in EU in the same year [1]. This sector is, however, responsible for a high share of greenhouse gases emissions (GHGs) and other pollutants, which are of particular relevance considering their impact at local level (i.e. port environment). Moreover, several long-term economic and energy scenarios foresee an increase of emissions in the near future, due to the rapid growth of the sector, which envisage a significant environmental challenges to overcome [2]. In recognition of the urgent need of addressing this issue, the International Maritime Organization (IMO) has undertaken decisive actions and set stringent goals, and the EU has put in place a significant number of initiatives towards the mitigation of the emissions of the maritime sector. A pivotal role within this context is that of hydrogen as fuel on ships [3]. Hydrogen owns indeed all the peculiar features of a clean fuel, with the potential to achieve a zero local-emission propulsion. In particular, Polymer Electrolyte Membrane (PEM) fuel cells (FCs) are emerging as the most promising technology for the exploitation of hydrogen on-board of ships.

In line with this context, in this paper three new vessel arrangements are proposed, whose powertrain consists in a hybrid PEMFC and batteries system. The three solutions are developed according to different design criteria, and on-board weights and spaces constraints are considered to allocate the components of the new hydrogen-based propulsion systems into the vessel. Thus, a comparative analysis is made among the three configurations and with the original Diesel one, in terms of hydrodynamic performances of the vessel.

1.1. PEMFC technology in maritime applications

The advancement of high-efficiency FC systems for ship propulsion is gaining a significant attention within the maritime industry, as well as within the scientific community. In particular, as emerging from literature, hydrogen PEMFC is considered the technology that currently offers the most promising solution. Few examples of recent works dealing with this topic are here reported for a reference.

A 100 kW PEMFC module integrated with a supercapacitors energy storage system and a DC/AC power converter for the marine propulsion was studied in Ref. [4]; in this paper, the authors highlighted that very interesting efficiencies, equal to 48% and 45% for the fuel cell and the overall system, respectively, were possible with this technology. Another study, carried out by Dall'Armi et al. [5], allowed to demonstrate that a hybrid PEMFC/Li-ion battery propulsion system could be effectively used for both a small RoRo vessel and a passenger ferry instead of the conventional fossil fuel powertrain; by means of a process simulation approach the authors evaluated the peak shaving services and verified that the proposed technical solution allowed a reduction of the fuel cell size, set equal to 120 kW instead of 206 kW of the main diesel engine. In the study of Rattazzi et al. [6], a time-dependent thermo-economic analysis devote to evaluate the optimal operating conditions of a PEMFC-based system for a 200 people ferry was carried out. The application of a 114 kW PEMFC–based auxiliary power plant on board an existing oceanographic vessel was investigated by Antonio Villalba-Herreros et al. [7]; the aim of the study was to estimate the reduction of the CO2 emissions by using this technology both in the port and near inhabited areas. Di Micco et al. [8] performed a techno-economic feasibility analysis on the replacement of 8.3 MW diesel engine with a PEMFC system on a chemical tanker ship. The authors presented a detailed methodology, aimed to estimate the volume and mass of the fuel cell system as well as of the hydrogen storage technologies respect to the conventional solution. Results highlighted that the fuel cell-based powertrain allowed to achieve 60% less volume and 56% less mass compared to the diesel engine. In Ref. [9], an optimization model coupled with a Monte-Carlo analysis was implemented to understand the influence of PEMFC, battery pack and hydrogen costs on the operation of a hydrogen-powered ferry with hybrid powertrain in a long-term. The results showed that the hydrogen cost is the most crucial parameter, in particular toward the end of the plant lifetime, when hydrogen consumption increases by up to 30%.

Against this background, it is possible to emphasise that the scientific literature on the subject is quite wide, but the issues to be demonstrated are numerous and some further analysis is still required.

1.2. Barriers for hydrogen in maritime propulsion

The use of hydrogen and fuel cell technology is seen as an inevitable strategy for decarbonising the maritime sector, but several feasibility studies are needed to demonstrate that the criticality of hydrogen can be overcome. One of the primary issues is related to the development of efficient power units. As mentioned above, and as emerging from literature, hydrogen PEMFCs offer a promising solution, but their scalability and power density still have to be improved. Another critical issue regards the on-board storage of hydrogen, especially considering large vessels requiring substantial energy outputs [10,11]. Safety is another main, crucial point. The handling of hydrogen on-board of ships pose engineering challenges, as hydrogen owns some risks which are inherently different from those associated to other fuels. This requires different on-board infrastructures, with respect to those in place on-board of conventional vessels. Moreover, safety protocols and an ad-hoc regulatory framework for hydrogen on ships are absent to date and, therefore, they must be developed before a hydrogen-fueled vessel could be actually adopted [12]. The economic viability of hydrogen propulsion systems represents another critical barrier. The cost of hydrogen production, especially if derived from renewable sources, as well as the cost of hydrogen technologies, are still not competitive with those related to conventional fuels today used in the maritime sector. Additionally, the high initial investment required for retrofitting existing vessels or building new hydrogen-powered ships poses financial challenges for shipowners and operators [13–17]. The lack of an adequate infrastructure in ports represents another significant limitation to the adoption of hydrogen in this sector. In fact, unlike conventional fuels, which benefit from well-established supply chains and bunkering procedures and infrastructures, those for hydrogen have to be developed and built yet.

1.3. Contribution of the study and novelty

Addressing the above-mentioned criticalities requires a multidisciplinary approach involving technological innovation, policy support, and industry collaboration. First of all, a lack of knowledge for the design/retrofitting design of vessels has to be filled [18,19]. Several open issues remain in these regards, as for instance the integration of fuel cell technologies with batteries [20]. Also, the architecture of hydrogen-fueled vessels has to be redefined or assessed, either in terms of internal space allocations and/or hull geometry. Hydrodynamics characteristics have to be then verified, in order to make the new vessels having the same sailing performance of the conventional ones. In this context, a comprehensive design methodology is developed in this work to define the concept design of a hydrogen-powered ferry for passenger

transport. The proposed methodological approach encompasses the following steps.

i) analysis of power and energy requirements for the original vessel;
ii) design of a hybrid fuel cell/battery powertrain and performance assessment over typical operational profiles;
iii) definition of the H_2 vessel layout by allocating the new components and rearranging on-board spaces;
iv) numerical simulation and validation of the hydrodynamic behavior of the new vessel design.

This procedure is based on an iterative routine, until to find an optimal converge solution. In this work, such a methodological approach is applied to a RoPax vessel, for which a new fuel cell/battery hybrid powertrain is meant to replace its original Diesel-engines system.

2. Materials and methods

Starting from a vessel propelled by conventional Diesel engines, in this work a new hydrogen-configuration is studied and analysed through a multidisciplinary approach involving: energy analysis, modelling and design of hybrid fuel cell/battery powertrains, design of the vessel internal layout, and computational fluid dynamics analysis of the hull in calm water conditions. The results have allowed to evaluate the actual feasibility of implementing hydrogen technologies on-board of the considered vessel.

2.1. The case study: RoPax vessel configuration and operation

The case study analysed in the present paper was developed as a scenario for experimentation in the framework of the EU-funded HORIZON 2020 project e-SHyIPS [21,22]. The vessel taken as scenario reference is the Fior Di Levante, a ship managed by the Greek operator Levante Ferries. Fior Di Levante is a RoPax vessel with roll-on roll-off features for the carriage of commercial vehicles and private cars with the provision to accommodate large number of passengers for shorter routes. It is representative of a main area of interest for the maritime passenger transportation within European countries [23]: the short sea shipping – mainly between coastal cities or island – with passenger monohull ferries providing daily services for interregional mobility. The analysed case study operates daily routes from the mainland port of Killini to the islands of Zakynthos, Kefalonia, and Ithaca. In addition to passenger accommodation and garage decks for cars and trucks, plenty of amenities are offered on-board: bars, restaurants, children's facilities, and a small shopping arcade. Table 1 reports the main features of the considered vessel.

In order to evaluate the energy and power demand of the ship, a typical/average operational profile is constructed on the base of statistical data provided by the shipping company. According to these data, which are summarized in Table 2, on a yearly basis, the total sailing time of the ship is of 7.56 h during an average day, while 9.15 h are spent at berth. Both the main and the auxiliary internal combustion engines (ICEs) run for the whole duration of the sailing, while at berth, the main ICEs run for approximately 12% of the time.

A single voyage lasts around 80 min, and it is performed in three stages, namely departure (5 min), full away (60 min), and arrival (15 min). The speed frequency of the ship during departure/arrival and full away stages is shown in Fig. 1. The power request by the main ICEs during sailing has been then retrieved by the available speed-power curve of sea trial.

By considering a Lower Heating Value (LHV) of 42.7 MJ/kg for the fuel (both LSFO and MGO), the average main ICEs efficiency results to be approximately equal to 26%. Thus, assuming this value and with the fuel consumption at berth known (i.e. 104 kg/h, Table 2), the constant power output of the main ICEs at berth, during their operation, was computed and found to be equal to 324.4 kW. As far as the auxiliary GenSets are concerned, these are assumed to operate at constant load during the whole operation of the ship (sailing and at berth), by delivering electrical power to a number of auxiliary utilities. In the original vessel

Table 1
Main features of the Fior Di Levante RoPax ferry.

Feature		Description
General	Type of ship	Steel monohull RoPax
Dimensions	LOA - BOA	118.80 m–20.00 m
	Max displacement	5730.93 GT
Operational profile	Routing type	costal/island navigation
	Routing specification	Ioanian Sea, West Greece
	Distance covered	17–22 nm per trip
	Service speed (max)	17.8 kn (19 kn)
	Travel frequency	5/6 trip per day
	Bunkering frequency	Twice a week (partial refueling)
Pa & freight	Max persons on board	1140 pax + 24 crew
	Car capacity	310 Private Cars or 32 Trucks + 130 Cars
	Garage areas	Deck 3 & open Deck 5
	Passenger accommodation	Deck 6 & open Deck 7
Propulsion & aux equipment	Main engines	2 × 3520 kW MAN B&W 16V28/32A
	Aux engines (GenSets)	4 × 650 kW MAN B&W 5L23/30H
	Machineries arrangement	Deck 1 and 2 under main garage
	Machinery room volume	1820 m^3
	Weight of machineries	150 tons (2.6% of max displacement)
Fuel tank capacities	LSFO volume	215 m^3
	MGO volume	165 m^3
	Total weight (tank + fuel)	335 tons (5.8% of max displacement)

Table 2
Ship's average daily operational profile.

Operation	Time [h]			Fuel consumption [kg/h]	
	Tot	Main ICEs	Aux ICEs	Main ICEs	Aux ICEs
Sailing	7.56	7.56	7.56	697	218
At berth	9.15	1.13	9.15	104	218

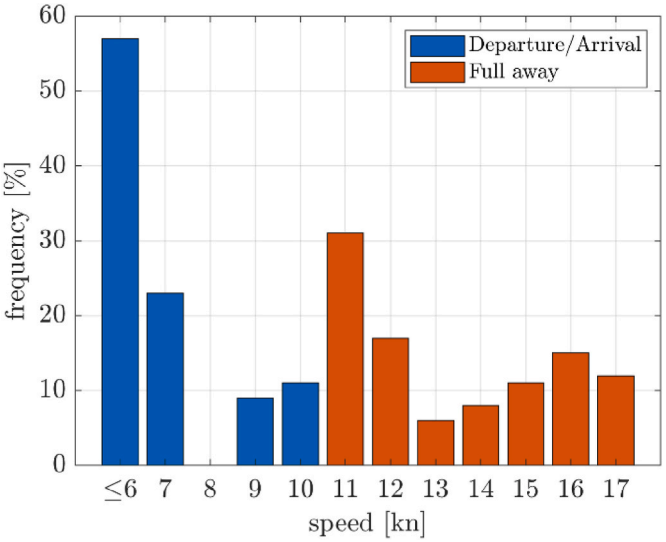

Fig. 1. Speed frequency profile for departure/arrival and full away stages of sailing.

configuration, the boiler runs on MGO and it has a 2000 kg/h of steam capacity, operating at a pressure of 7 bar at average 25% constant load. By this means, and assuming 80% of thermal efficiency, its related fuel consumption stands at 36 kg/h. In the new hydrogen-powered configuration of the ship instead, the boiler is assumed to be electrical, with power supplied by the auxiliary GenSets. Thus, considering a 98% of electrical efficiency, the electricity demand of the boiler corresponds to 349.9 kW. In order to compute the electric power request of all the other utilities, the remaining fuel consumption for the auxiliary ICEs is considered, this being obtained as the difference between the total amount (i.e. 281 kg/h, Table 2) and that for the boiler. Thus, assuming an ICE efficiency of 40% and 75% efficiency for the electric power generator, an overall 647.1 kW of electrical power demand is computed, this corresponding to an operation at 33.2% load for each of the four auxiliary ICEs.

The main results from this analysis are reported in Table 3, where the values reported for the main ICEs refer to a mechanical power, while those for the auxiliaries are meant to be electrical power.

2.2. Design of H_2 powertrain configurations

In the new hydrogen-powered configuration of the ship, the main ICEs and the auxiliary GenSets are replaced by a hybrid fuel cell/battery system, which has to provide both propulsion and auxiliary power. The hybrid unit is then connected to electric motors to propel the ship. An azimuthing propulsion system is assumed, where the electric drive motor is housed in a submerged pod outside the ship hull. In particular, two Azipod DO1250A units (rated power: 2 × 4.3 MW) from ABB [24] are considered as a reference for the present study.

The main requirement for the new H_2 vessel is that it has to accomplish the same operations and achieve the same performance of the original vessel. Therefore, the total electric power requested at the hybrid power unit (P_{tot}) is computed basing on the power demand of the original systems as provided in previous Section, according to the following general relation:

$$P_{tot} = P_{main\ ICEs}/\eta_{EM} + P_{boiler} + P_{AUX} \quad (1)$$

where $P_{main\ ICEs}$, P_{boiler} and P_{AUX} refer to the mechanical power output of the main ICEs, and the electric power consumption for boiler and other auxiliaries, respectively, as summarized in Table 3, while η_{EM} is the efficiency of the electric motor system, taken constant and equal to 90%, for the sake of simplicity. Note that the power P_{tot} that has to be supplied by the fuel cell and the battery to the electric motor (EM) is a function of the speed profile, during sailing, while it takes two different values during ship stay's at berth. Fig. 2 shows the electric power profile and the total energy demand during a single trip, requested by the electric motor in sailing conditions, while in Fig. 3 a breakdown of the energy demand is reported.

According to the considered operational profile, in sailing conditions the greatest share of energy has to be provided at a speed of 11 kn and at the highest speeds, i.e. 16-17 kn, of the ship. Moreover, the energy breakdown reveals that the greatest amount of energy is requested during full away, even though the share of energy requested by the hybrid power unit at berth is substantial (i.e. 27%).

Table 3
Power request for propulsion and auxiliaries.

Component	Mode	Power profile	Average power [kW]	Peak power [kW]
Main ICEs	Sailing: full away	f(speed)	2696.2	5193.5 @ 17 kn
	Sailing: departure/ arrival	f(speed)	608.9	1127.5 @ 10 kn
	At berth	f(time)	40.1	324.4
Auxiliaries: boiler	Sailing/At berth	constant	349.9	–
Other auxiliaries	Sailing/At berth	constant	647.1	–

On the base of the electric power/energy demand analysis, three H_2-based powertrain configurations are proposed, and the performance of each solution (i.e. H_2 consumption, average fuel cell efficiency) are estimated in order to provide an exhaustive framework of the potential use of hydrogen technologies on-board of the considered ferry. The three powertrain configurations share a common architecture, which is illustrated in Fig. 4; however, the size of each of the main components, i.e. fuel cell and battery systems, are selected according different design concepts, summarized in Table 4 and described in more details below.

The main assumption is that, in all cases, the fuel cell dynamic behavior is sufficiently fast to follow the load variations. This assumption is reasonable to the purpose of the present analysis, since the load is taken as composed of a series of steady operating points, rather than being made by an actual transient profile.

The first powertrain configuration assumes that the battery is of negligible capacity, that is, all propulsion and auxiliary power is supplied by the fuel cell system, during both sailing and at berth conditions. The fuel cell rated power is therefore set equal to the total ICEs power of the original vessel (Table 1).

The second configuration considers instead a battery pack of high capacity, which is conceived to fulfil the whole energy demand of the ship during the stay at berth. That is, the fuel cell provides alone the requested power for both propulsion and auxiliaries when sailing, while the battery gets depleted only at berth to cover alone the energy request. In this scenario, the battery pack is recharged overnight from an external source, therefore, this solution encompasses a plug-in architecture of the powertrain. Specifically, the computed total electric energy requested at berth, during a single day, is $E_{berth} = 9.53$ MWh. By assuming a 75% depth of discharge (DoD) for the battery and an overall discharge efficiency $\eta_b = 95\%$, the battery pack capacity results equal to 13.4 MWh, according to the following equation:

$$E_b = \frac{E_{berth}}{DoD\ \eta_b} \quad (2)$$

As far as the fuel cell size is concerned, this is defined considering the total electric power requested at 17 kn of speed (i.e. maximum power, see Table 2) increased by a contribution, to take into account the energy loss due to a DC/DC conversion. In fact, the fuel cell is assumed to be connected to the electric motors and the batteries through a DC/DC converter, with average efficiency $\eta_{DCDC} = 90\%$.

Finally, in the third powertrain configuration, the fuel cell is downsized with respect to the previous cases, and designed to fulfil the total power demand (propulsion and auxiliaries) up to 15 kn of speed. By considering the same DC/DC conversion efficiency mentioned before, its rated power results equal to 5.26 MW. In this scenario, the fuel cell supplies alone the requested energy when the ship is at berth. Moreover, this powertrain configuration is assumed to be non-plug-in, therefore the battery pack can be recharged only by the fuel cell during ship's operation. To accomplish this, and considering also that the battery has to cover the peak power demand at high speed during sailing, the fuel cell operating points and the battery pack capacity are designed in such a way to perform a charge sustaining-like behavior of the battery pack. Despite the development of an energy management strategy is out of the scope of the present study, the fuel cell set-points are selected to meet this criterion, according to the following approach.

- the fuel cell runs at constant power ($P_{FC,d/a}$) during departure/arrival operations, so as to provide the total requested power to the electric motors and to recharge the battery at the same time;
- in full away mode, the fuel cell follows the load up to a speed of the ship equal to 14 kn, that is, the battery pack is neither charged nor discharged under these conditions;

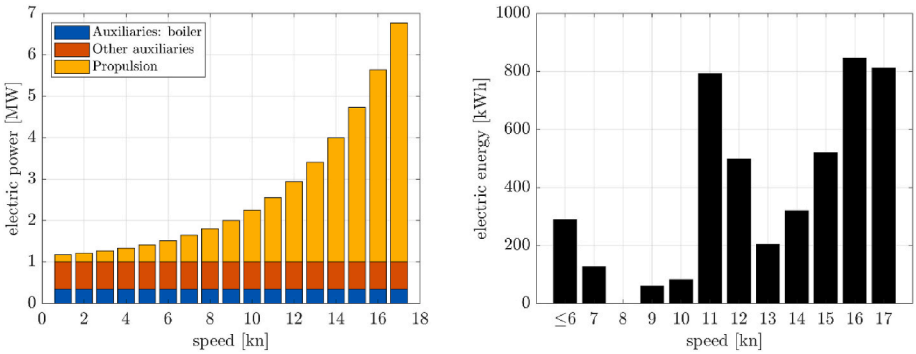

Fig. 2. Electric power (left) and total electric energy (right) demand at the hybrid power unit, as a function of the ship's speed, during sailing. The energy demand refers to a single trip.

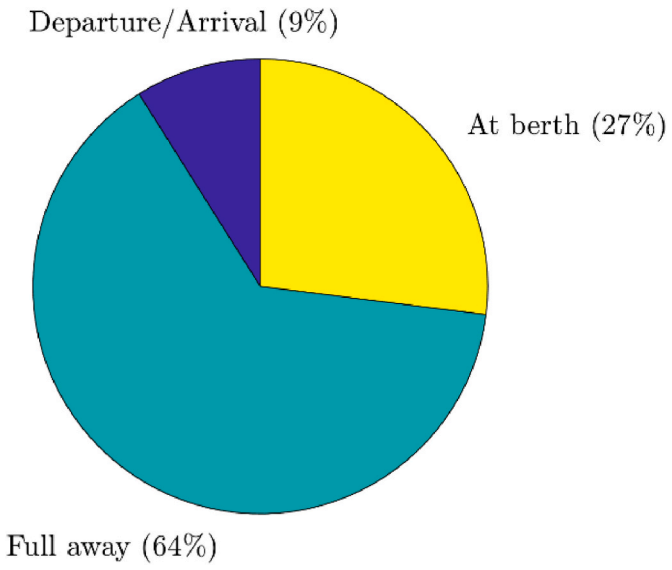

Fig. 3. Electric energy demand breakdown.

- the fuel cell power output is then set to a constant value ($P_{FC,high} = 4.80$ MW), close to its allowed maximum, during sailing at high speeds (i.e. above a speed of 14 kn), allowing for the battery pack to discharge to fulfil the power demand.

The battery pack size is evaluated by considering that a maximum of 75% of its energy capacity can be used to fulfil the maximum power request, $P_{tot,v_{max}}$ (i.e. electric power demand at a speed of 17 kn), for a

Table 4
H_2-based powertrain configurations.

Config. #	Description	FC rated power [MW]	Battery pack capacity [MWh]
1	- Battery neglected. - FC sized on total installed power of original vessel.	9.64	0
2	- Battery sized on a one-day *at berth* conditions. - FC sized on max power request during sailing.	7.52	13.4
3	- Battery sized for peak power requests. - FC sized on power requested for sailing at a speed of 15 kn	5.26	2.3

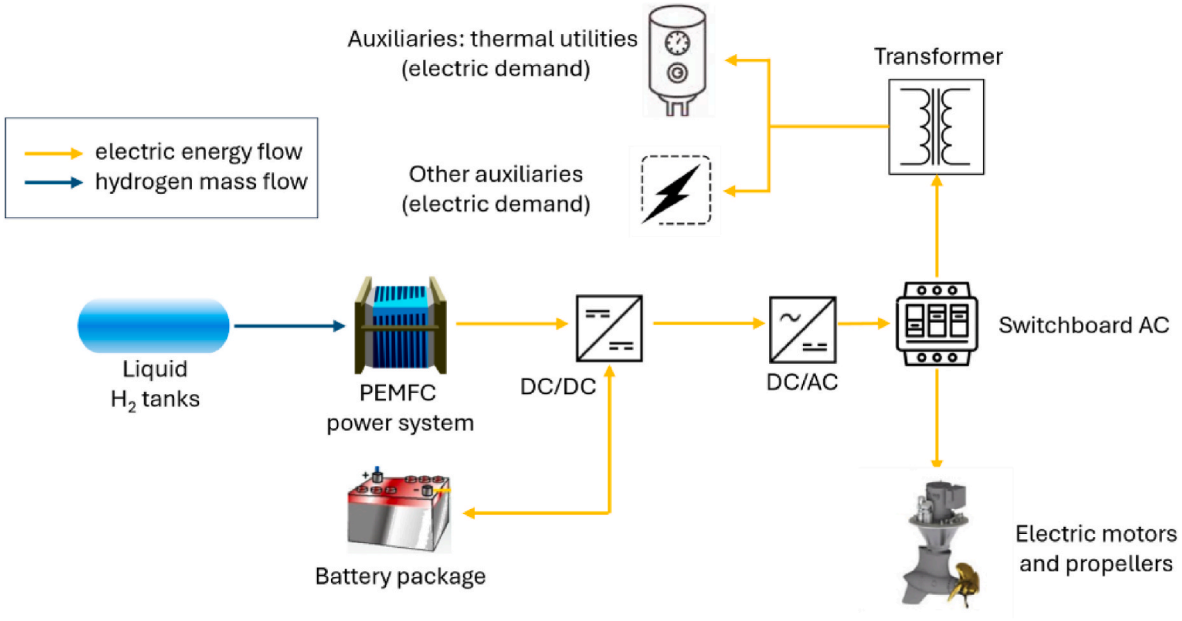

Fig. 4. Schematic representation of the general powertrain arrangement for the H_2-powered vessels.

whole day of operation, and by assuming the same discharge efficiency of previous configuration (i.e. 95%), that is:

$$E_b = \frac{P_{b,max}\Delta t_{v_{max}}}{DoD\,\eta_b} \tag{3}$$

where $\Delta t_{v_{max}}$ is the overall time spent sailing at maximum speed during a day of operation, and $P_{b,max}$ is the maximum discharge power achieved by the battery, which is given by:

$$P_{b,max} = P_{tot,v_{max}} - P_{FC,high}\eta_{DCDC} \tag{4}$$

The value for the fuel cell power output during departure/arrival is finally obtained by the following energy balance system of equations:

$$\begin{cases} E_{b,ch} = \sum_{i=1}^{n} P_{b,i}\Delta t_i\eta_b = \sum_{i=1}^{n}\left(P_{FC,d/a}\eta_{DCDC} - P_{tot,i}\right)\Delta t_i\eta_b \\ E_{b,disch} = \sum_{i=1}^{m} P_{b,i}\Delta t_i \Big/ \eta_b = \sum_{i=1}^{m}\left(P_{tot,i} - P_{FC,high}\eta_{DCDC}\right)\Delta t_i/\eta_b \\ E_{b,ch} = E_{b,disch} \end{cases} \tag{5}$$

where: $E_{b,ch}$ and $E_{b,disch}$ represent the net overall energy supplied by the fuel cell to the battery and the net overall energy provided by the battery to the electric motor, respectively; the indexes n and m are the number of powertrain operating points during departure/arrival and sailing at high speeds (i.e. 15-17 kn), respectively; Δt_i , $P_{b,i}$ and $P_{tot,i}$ are the time durations, battery power output and electric load request, for each i-th operative condition of the powertrain, respectively. As a result, a value of 3.84 MW if calculated for $P_{FC,d/a}$.

2.3. LincoSim: a virtual web towing tank tool

Thanks to the exceptional technological development of computational systems and numerical methodologies over the last 50 years, it has been possible to start talking about effective virtual towing tanks for some years now. Virtual towing tank means the computational transposition, or virtualization, of a real experimental measurement system such as the towing tank as conceived by Froude in 1870 [25]. It is easy to see how strategic such a tool is when economic and/or time resources are a strong constraint on the project, or when the main interest is to probe a wide range of possible variations in parameters with a series of hypothesis-testing investigations.

With the intention of investigating and identifying a series of practical prerequisites to support the emerging marine regulations for hydrogen-powered boats, it is strategic to be able to probe a wide range of design options for the identified hull types with reference to their future conversion to a hydrogen-based propulsion system. For this reason, LincoSim [26], i.e., the virtual ship tank developed in 2018 for the Horizon 2020 project LINCOLN [27], is a strategic tool to pursue this goal, since it allows to make a preliminary assessment of concept designs for the reconversion of pre-defined types of existing vessels with their operational profiles to hydrogen-based propulsion systems. A sketch of LincoSim architecture is provided in Fig. 5.

The interaction with the user is completely managed via a web interface, thus avoiding problems related to software installation and/or compatibility between versions, operating systems, or other components. The web interface is the access point of the web application that through its services (Application Programming Interfaces, APIs) manages the storage in a database and an advanced logic of operations. Through the interface, users can manage the geometries of the hulls accessible through a dedicated dashboard. After uploading the geometry – in a triangulated format such as stereolithography (stl) or Wavefront object (obj) – in view of the Computational Fluid Dynamics (CFD) simulation, a validation is performed, basically including a test of watertightness. Once a valid geometry is loaded, a simulation can be created requiring just a set of input data that characterize the physics of the flow, namely: the mass, the coordinates of the center of gravity, the moments of inertia, the speed of the hull, the initial water level, the initial hull trim angle and the water density. Once these inputs are defined, the platform can transparently submit the simulation to the selected High Performance Computing (HPC) cluster and the complete CFD workflow is then automatically managed form input to output data processing and visualization according to a selected given setup.

The underlying engine of the simulation setup can be defined in different ways by platform administrators, and it is currently based on a full open-source software stack. The CFD solver is provided by OpenFOAM [28] platform using the *interFoam* flow solver. The solver is based on the Navier Stokes equations for two incompressible, isothermal, and immiscible fluids, i.e., water and air. The density is the linear combination of the densities of the two fluids weighted using the phase-fraction variable which is set equal to 1 in water and 0 in air. An additional equation for phase variable is needed and Volume of Fluid (VoF) method is used to adequately evolve the air-water interface. More precisely, according to all practical industrial applications, the selected solver uses a Reynolds Averaged Navier-Stokes (RANS) equations approach so that turbulence is modelled with two additional algebraic equations. This modelling approach allows the user to obtain effective results with a reasonable computational complexity and time to result, that thanks to the usage of HPC clusters in LincoSim is limited at its minimum. The turbulence model selected is the *SST k-ω* [29,30], that is recognized to be effective in the marine field of application.

Equations are solved in the hull reference frame with a mean fluid flow set equal to the opposite of actual hull speed. The incoming flow is assumed as calm water field, i.e., without water waves. This assumption represents the virtualized counterpart of the towing tank resistance tests and represents a significant baseline testbed where the hull hydrodynamic behavior can be evaluated. The main results to be found are

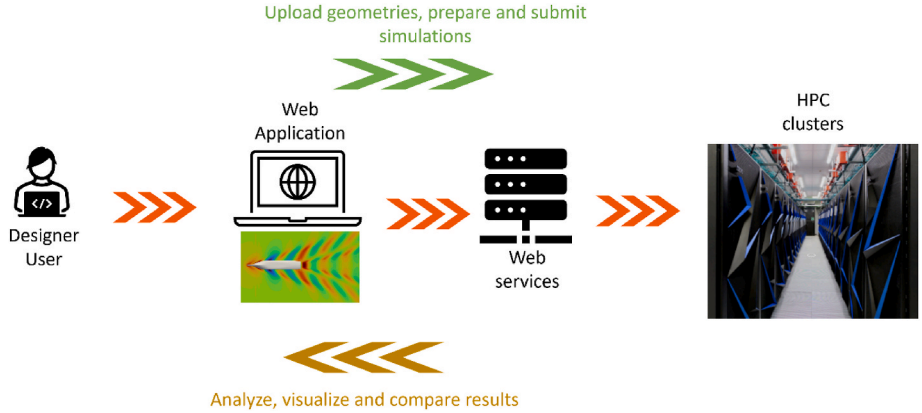

Fig. 5. Schematic of LincoSim architecture from the user workflow point of view.

usually the hull attitude and the resistance force. Hull attitude for the given configuration is typically described by two basic quantities. The first one is trim, the running angle of pitch motion of the hull, i.e., considering the mean flow along x direction in Fig. 6, the angle around y axis. The second one is the sinkage, which represents the value of heave motion (i.e., along z in Fig. 6) of the hull with respect to the water level. Since these quantities are not known a priori, the CFD simulations have additional unknowns representing the hull configuration, in particular 2 Degrees of Freedom (DoF). The solver is able to simultaneously find such values at equilibrium and the resulting steady flow field. From these results, the resistance force of the hull can be computed as a derived quantity. Additional interesting quantities can be derived as well, such as the area of hull wetted surface.

Following what suggested by the International Towing Tank Committee (ITTC) standards [31], for real physical towing tank studies, simulations for virtual towing tank have not been performed using real hull scale but using a reduced model scale. In physical towing tanks the model scale value is selected as large as possible for the size of the towing tank taking into consideration wall, tank blockage effect and finite depth effects as well as model mass and the maximum speed of the towing carriage. In the virtualized counterpart this is not strictly required but it is recognized to be a good practical approach to reproduce experimental/numerical comparable results and to better fit the limits of turbulence closures for a given computational complexity. Results found at model scale need to be rescaled to full size and this can be easily and quite reliably done using Froude similarity concepts.

The CFD simulation modelling requires the configuration of several physical and numerical inputs. As mentioned, LincoSim platform backend can automatically create such inputs starting from just the hull geometry file and few physical parameters related to the fluid dynamics condition of interest without the necessity to have any specific CFD competence. In particular, the computational mesh is automatically generated thanks to a standard procedure based on a background box with vertical refinement, additional horizontally refined boxes around the hull, and final geometry snapping stage to correctly represent the hull shape details. An illustrative example is shown in Fig. 7.

The background box accommodates the hull geometry plus significant buffer lengths in each direction, e.g., 3 hull lengths upstream and 7 lengths downstream the hull location respectively. Water and air physical properties are set according to user specific inputs or using default values.

The standardized and automated workflow implemented within LincoSim has been fully validated for calm water applications for mono and multi hull [32,33]. These hydrodynamic output quantities allow designers to rapidly compare and rank different hull and the usage of a web-based platform has been proven to improve designers' productivity [34]. For all of these reasons, this platform has been used in the present work to assess the hydrodynamic of the three designed vessel configurations, in particular with respect to the layout changes related to the hydrogen retrofitting.

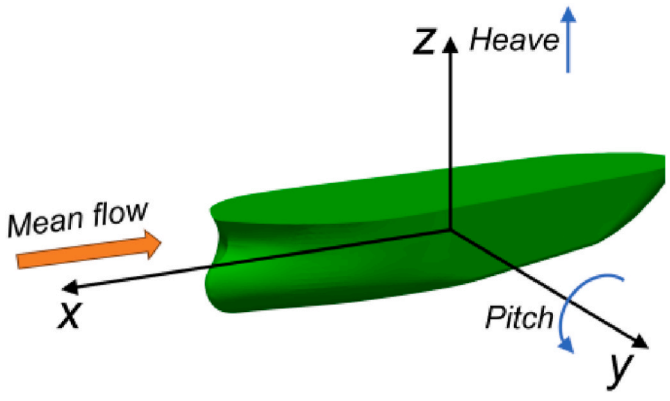

Fig. 6. Calm water simulation: mean flow and hull DoF.

3. Results and discussion

3.1. H_2 powertrain configurations performance and selection of components

In this work, the fuel cell system is modelled by means of an efficiency vs power output curve, that is constructed arbitrarily and taken as indicative of a typical PEM fuel cell behavior. In particular, the maximum efficiency has been set equal to 56 %, this value occurring at 25% of maximum load. By means of this performance curve, and with the fuel cell power output set-points defined (Fig. 8), the hydrogen consumption for each scenario is evaluated, as summarized in Table 5.

With the hydrogen consumption defined for each configuration, space and weight requirements have been then estimated. To this aim, and considering the FC rated power defined for each configuration (Table 4), a reference FC stack has been selected, this being the PEM HH_{BBB} model from the EU Project STASHH – *Standard-Sized Heavy-duty Hydrogen* [35], with 220 kW rated power, and having 0.15 kW/kg and 0.23 kW/L of gravimetric and volumetric power density. Therefore, 44, 34 and 24 modules are used for the three configurations, respectively.

As far as the hydrogen storage is concerned, the liquid technology is selected, in line with the general trend of today research in maritime applications. In spite of an increased system complexity, liquid hydrogen (LH2) provides indeed higher energy density than more conventional gaseous solutions, this being a crucial aspect for the implementation of hydrogen technologies on-board of a ship of relatively big size as the considered one, where a significant amount of hydrogen fuel has to be stored in a limited space, in order to not reducing the payload and limiting the bunkering frequency at the same time. Specifically, the features of the MAN Cryo LH2 Fuel Gas Supply System (FGSS) [36] are considered in this study as a reference to compute space and weight requirements in the proposed hydrogen-powered configurations of the ship, as reported in Table 6. The selected LH2 system has obtained the necessary certification of seaworthiness and it has been approved by classification society such as DNV, since there are no current IMO standards or regulations for LH2 fuel gas supply systems yet.

Regarding the battery pack of the ship, reference conservative data for a classical Li-Ion technology are assumed, that are: 150 Wh/kg and 100 Wh/L of gravimetric and volumetric energy density, respectively. Despite this being a simplified approach for taking into account the presence of the battery pack, it is sufficient for the scope of the present analysis, which targets at a preliminary estimation of space and weight requirements of the hybrid powertrain. The following Table 7 summarizes the needs in term of space and weight for the H_2-based propulsion system of the three cases, and the relative impact of each of the main components, expressed in percentage over the total.

The second configuration, with oversized battery pack, is the one characterized by the highest weight and volume requirements, while the other two are similar to each other.

3.2. H_2 vessel concept design

Market competitiveness of RoPax ferries highly depend on business needs in term of number of passengers, cars and trucks places available on-board as well as facilities and services offered [37]. For this reason, the design strategy pursued in the rearranging of the on-board technical spaces attempts to minimize the impact of new H_2 system adoption without modifying decks number, and hull shapes and with minor changes in term of vessel's center of gravity. To perform the feasibility of replacing the diesel-based powertrain with a H_2 PEMFC-based one, the mass and space requirements of the new on-board components are evaluated in comparison with the original ones. The availability in term of space and weight for the replacement of machineries is analysed in details (Table 1) and, in particular, it emerges that the main source of

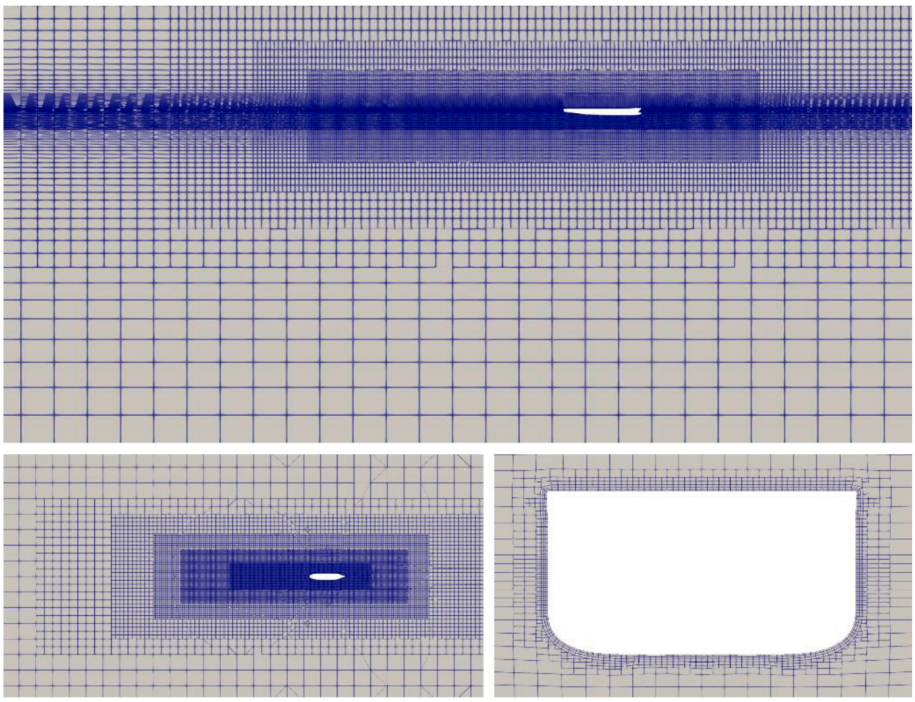

Fig. 7. Computational mesh view examples: symmetry plane (top), horizontal plane (bottom left) and details around hull with layering (bottom right).

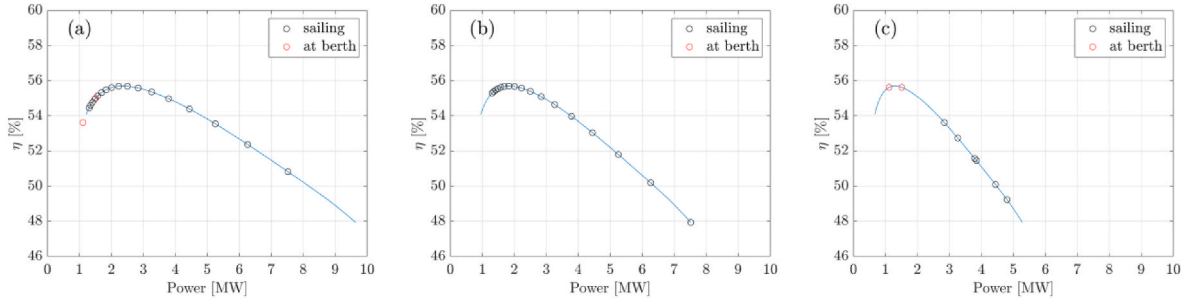

Fig. 8. Fuel cell power output set-points for config. #1 (a), config. #2 (b), and config. #3 (c).

Table 5
Hydrogen consumption per day [kg/day] for the three configurations.

	Config. #1	Config. #2	Config. #3
Sailing	1602	1648	1707
At berth	590	0	571
TOT	2192	1648	2278

Table 6
Main features of MAN Cryo's LH2 FGSS, single tank.

Gross volume [m^3]	95
Total weight [kg]	72500
H_2 capacity [kg]	2500
Gravimetric energy density [wt%]	3.45
Volumetric energy density [kg_{H2}/L]	0.0263

space left available for the implementation of the new components is the machinery room. Therefore, the three proposed designs locate LH2 tanks, gasification system and FC room on lower decks taking inspiration from the case study FreeCO2ast project, by Havyard Group ASA [38]. In particular, three LH2 storage systems (Table 6) are considered in each vessel configuration. The amount of stored hydrogen is then sufficient to allow for a three-day bunkering for configurations #1 and #3, and four-day bunkering when considering configuration #2, according to the identified requirements (Table 7). This option allows to maintain machinery rooms in the vessel lower decks as well as assuring a bunkering frequency which is in line with the Fior Di Levante operational profile. A 3D model was developed with the purpose of verifying the requirement in terms of volume, stability and performance. In Fig. 9, a 2D schematic representation of the vessel's layouts is shown, while in Fig. 10 the 3D visualization for the third vessel configuration is reported as an illustrative example.

Even if the design approach of configurations #1, #2, and #3 is the same – minimizing the changes on passenger compartment and garage area – the general arrangement of system compartment varies due to component dimensions. The three designs have in common the following features.

- LH2 storage tanks and FGSS are positioned on deck 1 symmetric on the central line. Ventilation path are designed in compliance with IGF code prescriptions.
- FC stacks are divided in two different rooms positioned on vessel side and placed from deck 2 to deck 4 (double height), to allow ventilation on the lateral side of the vessel and preventing down flooding in case of emergency/explosion.

Table 7
Space and weight requirements for the three H_2-based powertrain configurations.

	Config. #1				Config. #2				Config. #3			
	Weight		Volume		Weight		Volume		Weight		Volume	
	[tons]	[%]	[m^3]	[%]	[tons]	[%]	[m^3]	[%]	[tons]	[%]	[m^3]	[%]
Fuel cell	65.5	49.9	42.5	33.8	51.1	26.9	33.2	14.4	35.7	29.9	23.2	17.4
Battery	0.0	0.0	0.0	0.0	89.2	47.0	133.8	58.3	15.6	13.0	23.4	17.6
H_2 fuel	2.2	1.7	–	–	1.6	0.9	–	–	2.3	1.9	–	–
H_2 tank	63.6	48.4	83.3	66.2	47.8	25.2	62.6	27.3	66.1	55.2	86.6	65.0
TOT	131.3	100.0	125.8	100.0	189.7	100.0	229.5	100.0	119.7	100.0	133.1	100.0

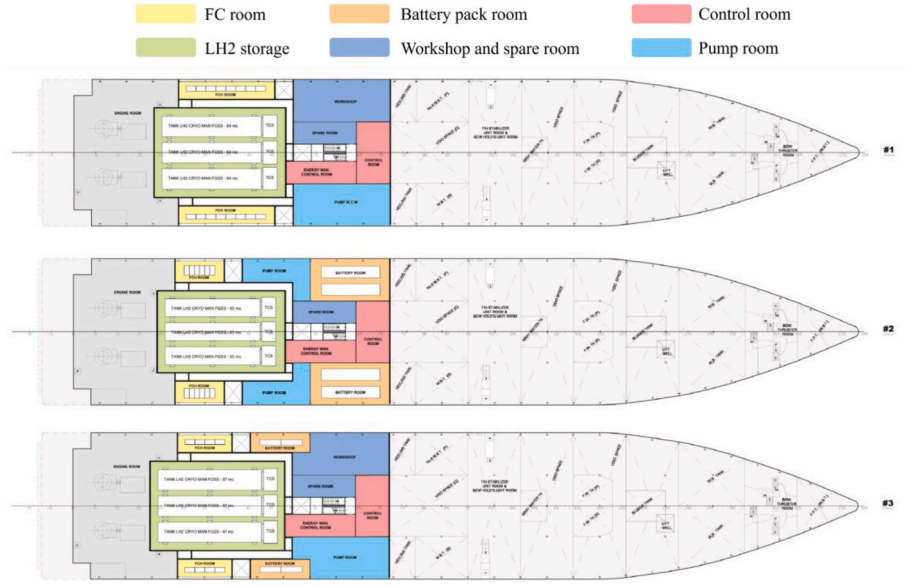

Figs. 9. 2D schematic layout of the three H_2-powered vessel's configurations.

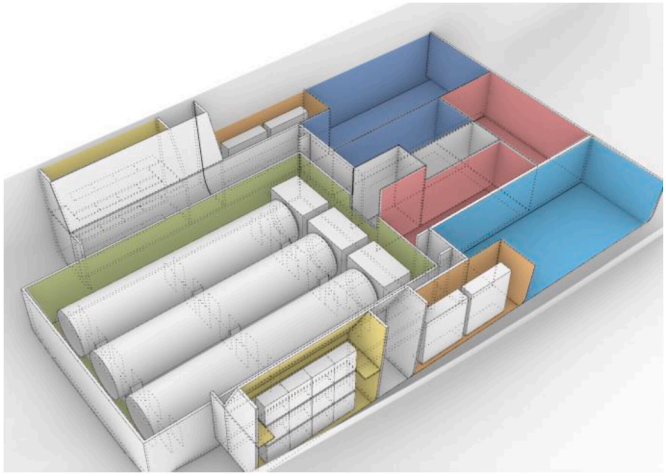

Figs. 10. 3D schematic layout of the H_2-powered vessel's configuration #3.

- Machinery corridors have air lock and double door compartment to avoid direct access from H_2 hazardous zone to not-H_2 hazardous zone
- Control room and energy management room are located centrally and accessible directly from crew distribution areas.

Then, differences in term of space arrangements are below highlighted.

- Design #1 allocates pump room, workshop room and spare room n.1 on deck 2. Due to the increasing volume need for LH2 tanks, the spare room n.2 is reallocated on deck 5 and hydraulic pump compartment is reallocated on deck 3, reducing the garage area of 105 m^2 (equal to 8 cars and 2 trucks place).
- Design #2 allocates pump room and spare room n.1 on deck 2. Due to the increasing volume need for H_2 system and batteries, the workshop and the spare room n.2 are reallocated on deck 5, while hydraulic pump compartment is reallocated on deck 3, reducing the garage area of 156 m^2 (equal to 18 cars and 2 trucks place).
- Design #3 allocates pump room, workshop room and spare room n.1 on deck 2. Due to the increasing volume need for LH2 tanks, the spare room n.2 is reallocated on deck 5 and hydraulic pump compartment is reallocated on deck 3, reducing the garage area of 105 m^2 (equal to 8 cars and 2 trucks place). Furthermore, the workshop room is slightly smaller than business use case (−12% of surface available)

For the three defined configurations, the following loading conditions are examined for the purpose of assessing whether the stability criteria are met and to provide input data for CFD simulations.

- *Full load*: ship in the fully loaded departure condition with cargo homogeneously distributed throughout all the cargo spaces and with full stores and fuel.
- *Mid load*: ship in the fully loaded departure condition with cargo homogeneously distributed throughout all the cargo spaces and with 10% of stores and of fuel, as represented by the last round voyage before bunkering.

According to loading condition and component distribution, the physical proprieties of the three vessel configurations are described with displacement, center of gravity, mass and moment of inertia.

3.3. Hydrodynamic calm water numerical analysis

The drag resistance in calm water conditions is predicted for the three vessel's configurations and compared to that for the original vessel. Fig. 11 shows the evaluated drag force profiles, as a function of the speed of the ship, in full load and mid load conditions, while in Fig. 12 the same results are rearranged, for the baseline and the hybrid configurations, to perform a comparison of the drag curves between full and mid loads, for each specific case.

The general trend of the drag resistance over speed remains substantially the same, among all vessel's configurations, when considering both full and mid load conditions. This is a positive result, since it provides that all the designed hydrogen-powered vessel's layouts do not lead to any disadvantage in terms of hydrodynamic performance. In particular, above the maneuvering speed (i.e. 6 kn), the baseline Diesel-configuration seems to achieve slightly better performance in full load conditions, while in mid load conditions an opposite behavior is observed, with all the hybrid vessel's configurations exhibiting a reduced drag resistance. At the lowest speed of the ship instead, namely 6 kn, the baseline Diesel-configuration provides better drag resistance performance with respect to all hybrid configurations and in both load conditions. Fig. 13 shows the relative percentage difference, for the drag resistance, computed for all hybrid configurations with respect to the baseline one. Except for the lowest considered speed, where a difference up to 17% is found, the deviation for the drag force experienced by the hybrid configurations with respect to the Diesel one is generally within the $-8/+5\%$ of range.

As far as the comparative analysis of full and mid load conditions, for each vessel's configuration (Fig. 12), the results from the numerical simulations show that a major difference is observed only at the highest speeds for the baseline configuration, while significant differences in terms of drag force occur also at intermediate speeds for the H_2-based configurations. Inspecting the relative percentage differences from Fig. 13, the maximum difference between full and mid load conditions for the baseline configuration is approximately equal to 8% at maximum speed, while for the hydrogen-powered vessels this maximum stands in the range 11–16% and it is found to be at intermediate speed (i.e. 11 kn) for configurations #1 and #3, and at the lowest speed for configuration #2.

It has to be noted that the intermediate speed at which the greatest differences between full and mid load drag resistance is generally experienced for the hydrogen vessels (i.e. 11 kn) is the most frequent speed condition during sailing in full away (Fig. 1), and also it corresponds to one of the most energy demanding operative condition (Fig. 2). This emphasizes the need of taking into full account mid load conditions as well in the design process of new fuel cell/hybrid layouts, since the hydrodynamic performance of the vessel may vary significantly with respect to full load conditions.

Next, in Figs. 14 and 15, the obtained sinkage and trim of the vessel are presented, for all analysed configurations, under both full and mid load conditions.

From these results, some differences between the baseline configuration and the hybrid ones is obtained, even though no critical behaviors are found for the new vessel configurations, overall.

The sinkage of the hybrid vessels is almost 1.5 m higher than the value for the Diesel one, along the whole span of velocities, and in both full and mid load conditions. This may be ascribed to the slightly different total weight of the vessel configurations, with the baseline one being the heaviest. As far as the dynamic trim is concerned, the obtained profiles for the hybrid configurations are well in line to each other and they only slightly deviate from that of the baseline configuration, in full load conditions. Instead, an opposite sign is found between the trim values of hybrid and Diesel configurations when mid load conditions are considered. The obtained values of the dynamic trim for the hybrid configurations are, however, still small (below 1°) and, therefore, it can be concluded that the new proposed layouts for these configurations do not affect significantly the hydrodynamic response of the vessel.

4. Conclusions

In this paper, a comprehensive methodological approach is proposed and applied to support the retrofit design process of a passenger ferry into a hydrogen-powered configuration. Energy and power requirements of the vessel are retrieved and a typical operational profile is reconstructed from available data. These serve as a basis to size the new power unit components and the energy storage system. In particular, three different layout configurations are explored, with the aim of understanding the impact of a different arrangement of components onboard, given by different hybridization approaches, on the overall hydrodynamic response of the vessel. Therefore, a virtual towing tank environment is used to simulate and assess the vessel behavior under calm water conditions.

Findings from this analysis show that.

i) from a vessel's layout point of view, all H_2 configurations are affected by a slight payload reduction. Space availability is in fact an issue, especially to allocate the bulky hydrogen storage tanks. Despite this, the proposed solutions are still competitive and comparable with the original one.
ii) Overall, minimal but not negligible differences are found among the baseline Diesel and the new hydrogen vessels configurations, in terms of hydrodynamic response.
iii) The hydrodynamic performance of the three H_2-based configurations are very close to each other in both full and mid load conditions.

These results points out the need of choosing the best hybrid configuration for the vessel mainly on the base of use-case requirements

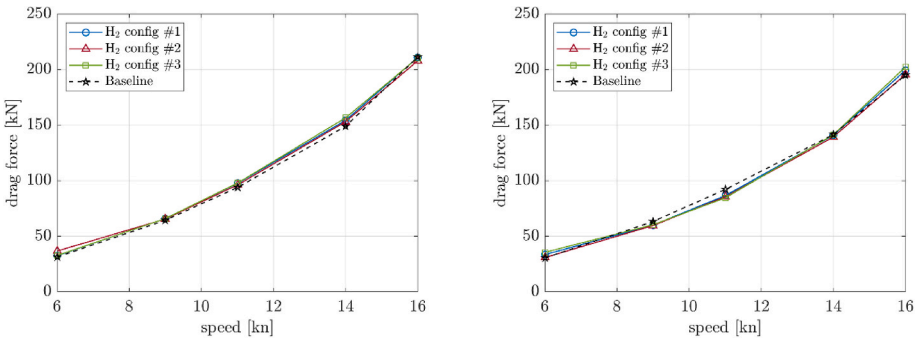

Fig. 11. Drag resistance profile for all vessel's configurations in Full load (left) and Mid load (right) conditions.

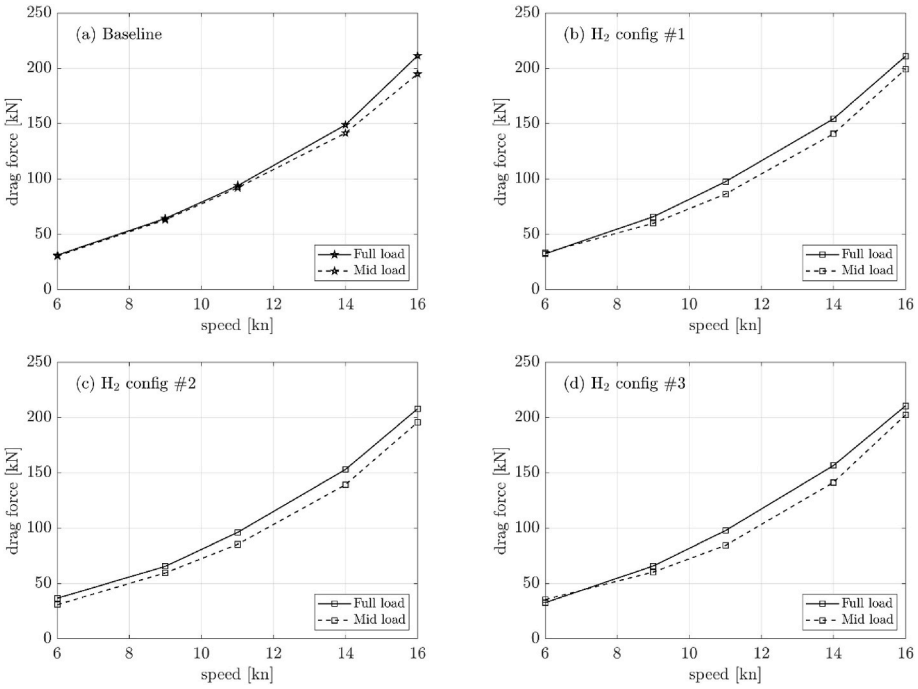

Fig. 12. Drag resistance profile comparison between Full load and Mid load conditions: (a) Baseline configuration, (b) H_2 configuration #1, (c) H_2 configuration #2, (d) H_2 configuration #3.

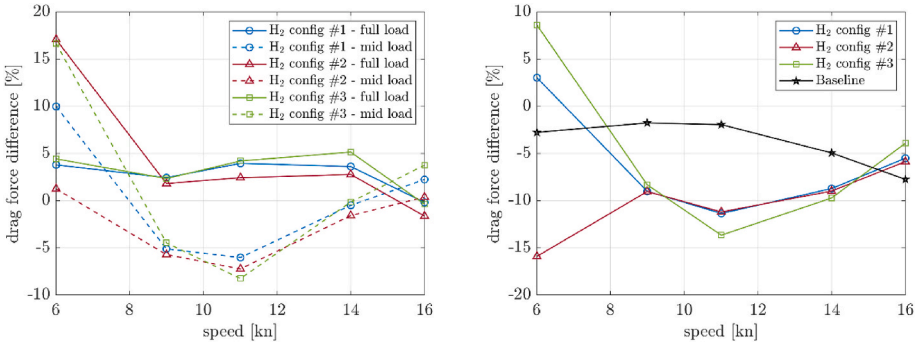

Fig. 13. Drag resistance relative difference: between baseline and hybrid configurations (left), between full and mid load conditions for each configurations (right).

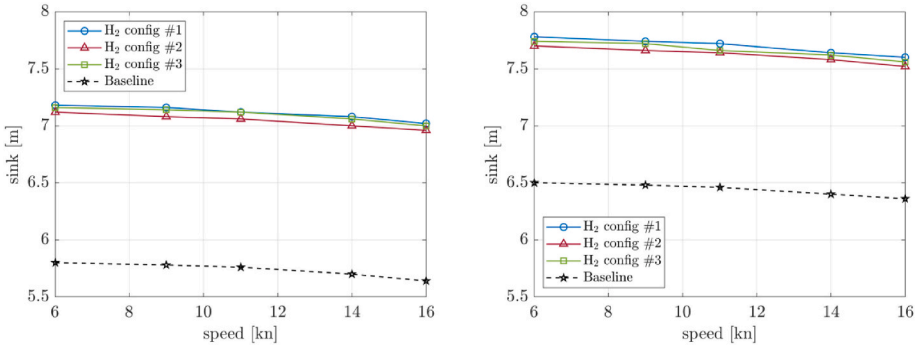

Fig. 14. Sink profile for all vessel's configurations in Full load (left) and Mid load (right) conditions.

rather than hydrodynamic aspects, but also that mid load operating conditions get relevance in the optimal retrofit design process of the new hybrid vessel.

CRediT authorship contribution statement

G. Di Ilio: Writing – review & editing, Writing – original draft, Visualization, Validation, Methodology, Investigation, Formal analysis, Conceptualization. **A. Bionda:** Writing – original draft, Project

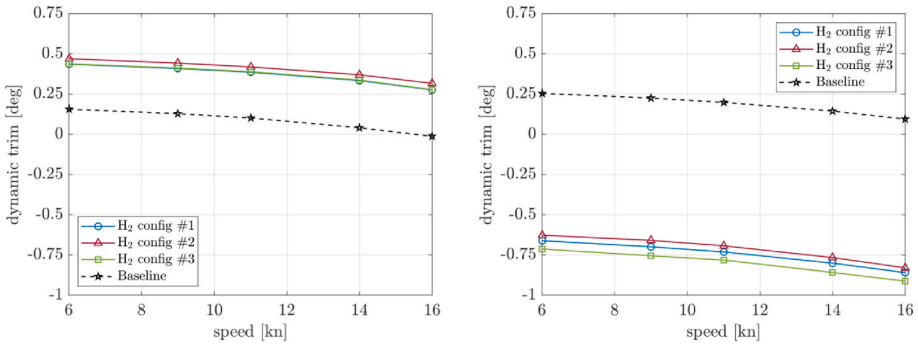

Fig. 15. Dynamic trim profile for all vessel's configurations in Full load (left) and Mid load (right) conditions.

administration, Investigation, Formal analysis. **R. Ponzini:** Writing – original draft, Software, Methodology, Investigation, Formal analysis. **F. Salvadore:** Writing – original draft, Software, Methodology, Investigation, Formal analysis. **V. Cigolotti:** Supervision, Formal analysis. **M. Minutillo:** Supervision, Formal analysis. **C. Georgopoulou:** Validation, Formal analysis. **K. Mahos:** Validation, Supervision, Data curation.

Declaration of competing interest

The authors declare that they have no known competing financial interests or personal relationships that could have appeared to influence the work reported in this paper.

Acknowledgments

This research has received funding from the Fuel Cells and Hydrogen 2 Joint Undertaking (now Clean Hydrogen Partnership) under grant agreement No 101007226, project e-SHyIPS - Ecosystemic knowledge in Standards for Hydrogen Implementation on Passenger Ship. This Joint Undertaking receives support from the European Union's Horizon 2020 Research and Innovation programme, Hydrogen Europe and Hydrogen Europe Research.

References

[1] Eurostat. Maritime passenger statistics. https://ec.europa.eu/eurostat/statistics-explained; 2023. accessed April 2024.
[2] International Maritime Organization (IMO). Fourth greenhouse gas study. https://www.imo.org/en/OurWork/Environment/Pages/Fourth-IMO-Greenhouse-Gas-Study-2020.aspx; 2020. accessed April 2024.
[3] Pfeifer A, Prebeg P, Duic N. Challenges and opportunities of zero emission shipping in smart islands: a study of zero emission ferry lines. eTransportation 2020;3:100048. https://doi.org/10.1016/j.etran.2020.100048.
[4] Pietra A, Gianni M, Zuliani N, Malabotti S, Taccani R. Experimental characterization of a PEM fuel cell for marine power generation. E3S Web Conf. 2022;334:05002. https://doi.org/10.1051/e3sconf/202233405002.
[5] Dall'Armi C, Micheli D, Taccani R. Comparison of different plant layouts and fuel storage solutions for fuel cells utilization on a small ferry. Int J Hydrogen Energy 2021;46:13878–97. https://doi.org/10.1016/j.ijhydene.2021.02.13.
[6] Rattazzi D, Rivarolo M, Massardo AF. An innovative tool for the evaluation and comparison of different fuels and technologies onboard ships. E3S Web Conf. 2021;238. https://doi.org/10.1051/e3sconf/202123808001.
[7] Villalba-Herreros A, Gómez MR, Morán JL, Leo TJ. Emissions and noise reduction on-board an oceanographic vessel thanks to the use of proton-exchange membrane fuel cells. Proc Inst Mech Eng Part M J Eng Marit Environ 2020. https://doi.org/10.1177/1475090219858819.
[8] Di Micco S, Mastropasqua L, Cigolotti V, Minutillo M, Brouwer J. A framework for the replacement analysis of a hydrogen-based polymer electrolyte membrane fuel cell technology on board ships: a step towards decarbonization in the maritime sector. Energy Convers Manag 2022;267:115893. https://doi.org/10.1016/j.enconman.2022.115893.
[9] Dall'Armi C, Pivetta D, Taccani R. Uncertainty analysis of the optimal health-conscious operation of a hybrid PEMFC coastal ferry. Int J Hydrogen Energy 2022;47:11428–40. https://doi.org/10.1016/j.ijhydene.2021.10.271.
[10] Ustolin F, Campari A, Taccani R. An extensive review of liquid hydrogen in transportation with focus on the maritime sector. J Mar Sci Eng 2022;10:1222. https://doi.org/10.3390/jmse10091222.
[11] Taccani R, Malabotti S, Dall'Armi C, Micheli D. High energy density storage of gaseous marine fuels: an innovative concept and its application to a hydrogen powered ferry. Int Shipbuild Prog 2020;67:33–56. https://doi.org/10.3233/ISP-190274.
[12] Aarskog FG, Hansen OR, Strømgren T, Ulleberg Ø. Concept risk assessment of a hydrogen driven high speed passenger ferry. Int J Hydrogen Energy 2020;45:1359–72. https://doi.org/10.1016/j.ijhydene.2019.05.128.
[13] Mojarrad M, Zadeh M, Rødseth KL. Techno-economic modeling of zero-emission marine transport with hydrogen fuel and superconducting propulsion system: case study of a passenger ferry. Int J Hydrogen Energy 2023;48:27427–40. https://doi.org/10.1016/j.ijhydene.2023.03.438.
[14] Mojarrad M, Thorne RJ, Rødseth KL. Technical and cost analysis of zero-emission high-speed ferries: retrofitting from diesel to green hydrogen. Heliyon 2024;10:e27479. https://doi.org/10.1016/j.heliyon.2024.e27479.
[15] Trillos, J.C.G., Wilken, D., Brand, U., Vogt, T., "Life Cycle Assessment of a Hydrogen and Fuel Cell RoPax Ferry Prototype", in: S. Albrecht et al. (eds.), Progress in Life Cycle Assessment 2019, Sustainable Production, Life Cycle Engineering and Management, Springer, https://doi.org/10.1007/978-3-030-50519-6_2.
[16] Temiz M, Dincer I. Techno-economic analysis of green hydrogen ferries with a floating photovoltaic based marine fueling station. Energy Convers Manag 2021;247:114760. https://doi.org/10.1016/j.enconman.2021.114760.
[17] Guven D, Kayalica MO. Environmental and economic assessment of hydrogen-powered ferries for inland transportation. Ocean Eng 2024;301:117556. https://doi.org/10.1016/j.oceaneng.2024.117556.
[18] Dall'Armi C, Micheli D, Taccani R. Comparison of different plant layouts and fuel storage solutions for fuel cells utilization on a small ferry. Int J Hydrogen Energy 2021;46:13878–97. https://doi.org/10.1016/j.ijhydene.2021.02.138.
[19] Minutillo M, Cigolotti V, Di Ilio G, Bionda A, Boonen E-J, Wannemacher T. Hydrogen-based technologies in maritime sector: technical analysis and prospective. E3S Web Conf. 2022;334. https://doi.org/10.1051/e3sconf/202233406011.
[20] Mylonopoulos F, Boulougouris E, Trivyza NL, Priftis A, Cheliotis M, Wang H, Shi G. Hydrogen vs. Batteries: comparative safety assessments for a high-speed passenger ferry. Appl Sci 2022;12:2919. https://doi.org/10.3390/app12062919.
[21] H2020 EU Project, FCH-04-2-2020, e-SHyIPS – ecosystemic knowledge in standards for hydrogen implementation on passenger ship, doi:10.3030/101007226.
[22] Ansaloni, G.M.M., Bionda, A., & Rossi, M. "EcoDesign strategies for zero-emission hydrogen fuel vessels scenarios", in: 2022 7th international conference on smart and sustainable technologies (SpliTech2022), IEEE.
[23] European Commission. Directorate-General for Mobility and Transport, EU transport in figures: statistical pocketbook. Publications Office of the EU; 2020.
[24] ABB Azipod electric propulsion. Available online: https://new.abb.com/marine/systems-and-solutions/dynafin/azipod#compact (accessed on 24 July 2023).
[25] Slade S. "History and technology: towing tank tests," NavWeaps: naval weapons, naval technology and naval reunions. Available at: http://www.navweaps.com/index_tech/tech-010.php; 19 December 1998.
[26] Salvadore F, Ponzini R. LincoSim: a web based HPC-cloud platform for automatic virtual towing tank analysis. J Grid Comput 2019;17(4):771–95. https://doi.org/10.1007/s10723-019-09494-y. Springer Science and Business Media LLC.
[27] LINCOLN project. https://cordis.europa.eu/project/id/727982; 2020.
[28] Weller HG, Tabor G, Jasak H, Fureby C. A tensorial approach to computational continuum mechanics using object-oriented techniques. Comput Phys 1998;12(6). https://doi.org/10.1063/1.168744.
[29] Menter F, Carregal Ferreira J, Esch T, Konno B, Germany AC. The SST turbulence model with improved wall treatment for heat transfer predictions in gas turbines. In: Proceedings of the international gas turbine congress; 2003. p. 2–7.
[30] Menter FR, Kuntz M, Langtry R. Ten years of industrial experience with the SST turbulence model. In: Proceedings of the fourth international symposium on turbulence, heat and mass transfer; 2003. p. 625–32. Antalya, Turkey.
[31] ITTC recommended procedures and Guidelines 7.5-02 -02-02. Available at: https://ittc.info/media/1219/75-02-02-02.pdf; 2008.
[32] Ponzini R, Salvadore F, Begovic E, Bertorello C. Automatic CFD analysis of planing hulls by means of a new web-based application: usage, experimental data

comparison and opportunities. Ocean Eng 2020;210:107387. https://doi.org/10.1016/j.oceaneng.2020.107387.
[33] Salvadore F, Ponzini R, Duque JH, Reinaldos CA, Soler JM. CFD analysis of a multiplatform catamaran by means of a web-based application: experimental data comparison for a fully automated analysis process. Appl Ocean Res 2021;116:102886. https://doi.org/10.1016/j.apor.2021.102886.
[34] Salvadore F, Ponzini R, Arlandini C. Improving the productivity of hull designers with HPC in the cloud: the LincoSim experience. In: IEEE international conference on systems, man and cybernetics (SMC); 2019. https://doi.org/10.1109/smc.2019.8914462.
[35] H2020 EU Project, FCH-01-4-2020, StasHH – standard sized FC module for Heavy duty applications, doi: 10.3030/101005934.
[36] MAN Cryo, Cryogenic solutions for onshore and offshore applications. Datasheet. Available online: https://www.man-es.com/docs/default-source/document-sync-archive/man-cryo-eng.pdf?sfvrsn=f1030ce2_3 (accessed on 24 July 2023).
[37] Zis TP, Psaraftis HN, Tillig F, Ringsberg JW. Decarbonizing maritime transport: a Ro-Pax case study. Research in Transportation Business & Management 2020;37:100565.
[38] Osnes K. Havyard Group ASA FreeCO2ast. Available online: https://www.gceocean.no/media/2677/freeco2ast-kristian-osnes.pdf. [Accessed 16 June 2023].